Supporting material

Membrane permeation induced by aggregates of human islet amyloid polypeptides

Chetan Poojari
Forschungszentrum Jülich GmbH,
Institute of Complex Systems: Structural Biochemistry (ICS-6),
52425 Jülich, Germany

Dequan Xiao
Department of Chemistry,
Yale University
New Haven, CT 06520, USA

Victor S. Batista*
Department of Chemistry,
Yale University
New Haven, CT 06520, USA

Birgit Strodel*
Forschungszentrum Jülich GmbH,
Institute of Complex Systems: Structural Biochemistry (ICS-6),
52425 Jülich, Germany

Institute of Theoretical and Computational Chemistry,
Heinrich Heine University Düsseldorf, 40225 Düsseldorf, Germany

*Corresponding Authors: victor.batista@yale.edu; b.strodel@fz-juelich.de

DPPG bilayer setup.
The PACKMOL package (1) was used to build a DPPG bilayer patch of 256 lipids with 128 lipids in each leaflet. The DPPG bilayer patch was solvated with 9,888 SPC water molecules and 256 Na^+ ions were added to neutralize the negatively charged DPPG molecules with each ion taking the place of a randomly chosen water molecule. The resulting DPPG bilayer system contained 42,208 atoms in a simulation box with dimensions of 8.6 × 8.6 × 8.0 nm^3 . The system was simulated for 100 ns at 323 K using a Nose-Hoover thermostat to regulate the temperature along with semiisotropic Parrinello-Rahman pressure coupling. The bilayer normal z-direction and xy-plane were coupled separately with a time constant of 2 ps maintaining a constant pressure of 1 bar independently in all directions. An isothermal compressibility of 4.5 × 105 bar^{-1} was applied in all box dimensions.

DPPG monolayer setup.
DPPG monolayers were built from the DPPG bilayer system by separating the two leaflets (2). The lower leaflet was moved in the positive z-direction while the upper leaflet was displaced in the negative *z*-direction until the separation between both membrane surfaces was 5.4 nm. Thus, the resulting system consisted of two monolayers with 128 DPPG lipids per layer separated by a central layer, which was filled with 11,389 SPC water molecules and 256 Na^+ ions. The complete DPPG monolayer system included 47,271 atoms within the simulation box of dimensions 8.6 × 8.6 × 16.0 nm^3. The large box length in the *z*-direction is necessary to create a vacuum region above and below the lipid tails of the upper and lower monolayer, respectively, to avoid any interactions between tail atoms of the two monolayers. A representative configuration of the DPPG monolayer system is shown in Fig. S1. This system was simulated for 100 ns at 323 K using a Nose-Hoover thermostat to regulate the temperature with a time constant of 1 ps. To control the pressure, a surface tension pressure coupling scheme with a time constant of 4 ps was employed (3). An isothermal compressibility of 4.5 × 105 bar^{-1} was applied in the lateral *x* and *y*-directions, while the compressibility was set to zero in the *z*-direction to prevent box contraction.

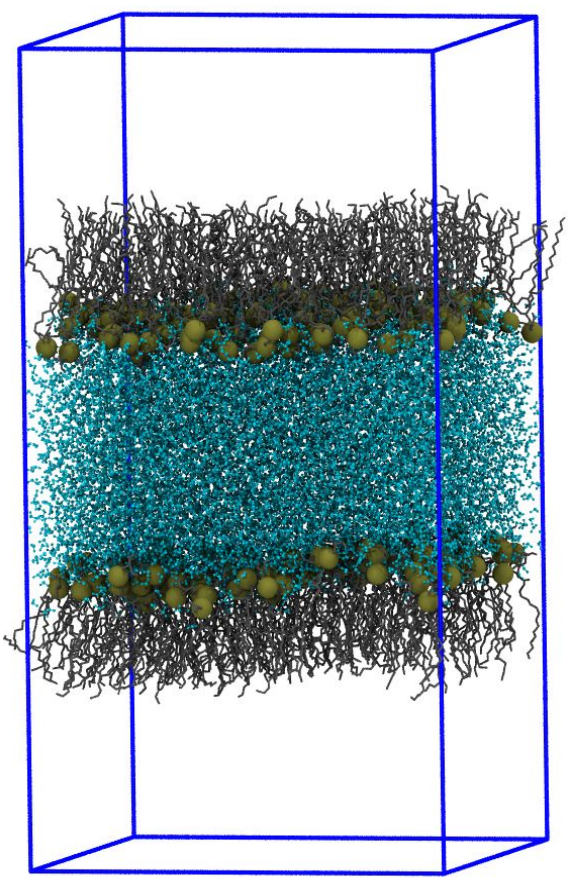

Figure S1: Snapshot showing the DPPG monolayer-water system. The monolayer phosphorus atoms (tan) are shown as van der Waals spheres, lipid tails (gray) as licorice and water molecules (blue) are shown as CPK. The simulation box is drawn to emphasize the empty space representing the air above and below the lipid tails in the upper and lower monolayer, respectively.

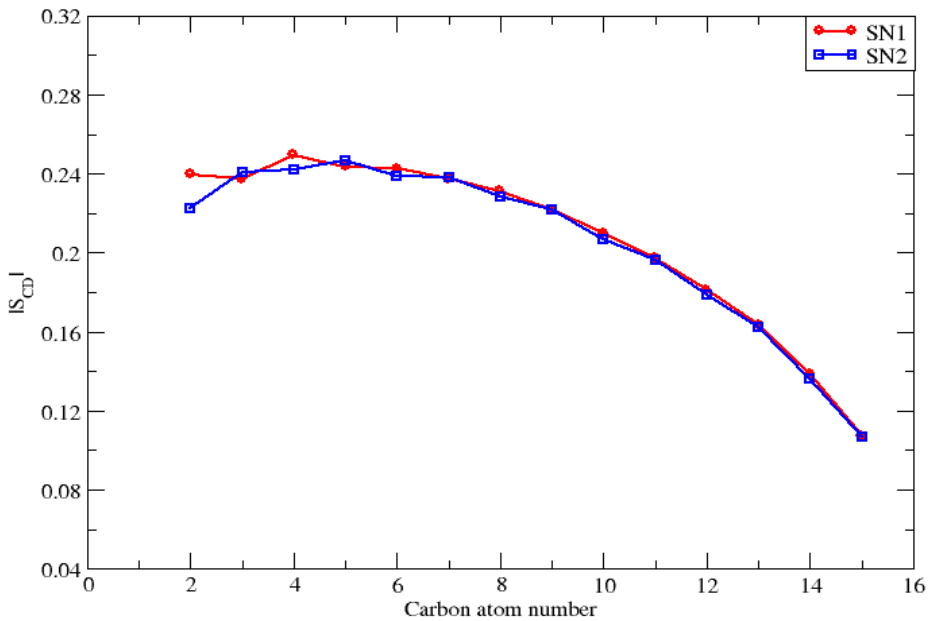

Figure S2: Time-averaged order parameter $|S_{CD}|$ of the sn-1 and sn-2 lipid chains obtained from a 100 ns MD simulation of a peptide-free DPPG bilayer.

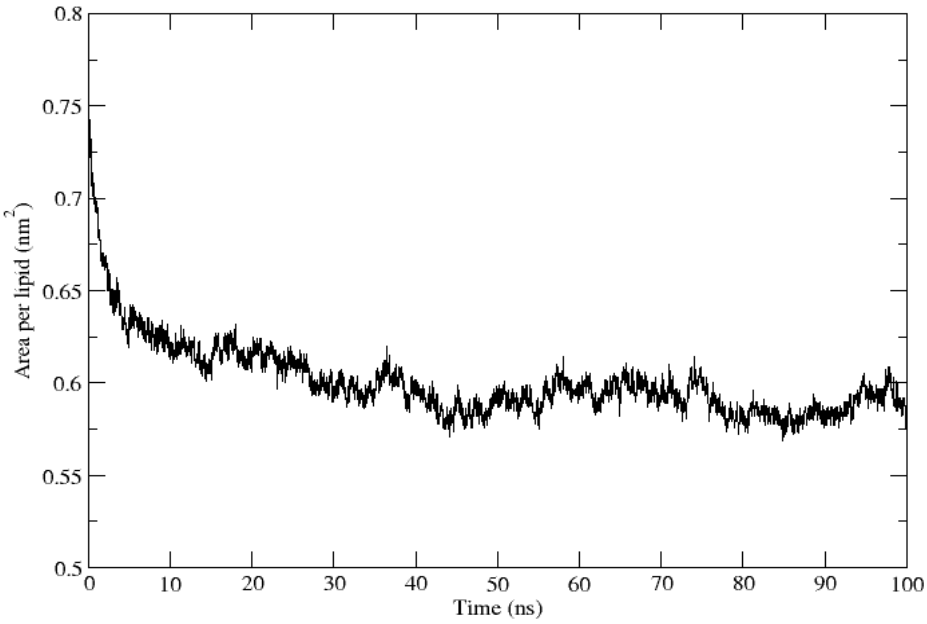

Figure S3: Area per lipid as a function of time as obtained during a 100 ns MD simulation of a peptide-free DPPG lipid bilayer.

Sum frequency generation spectrum calculations

The *psp* effective second-order susceptibility for the *q*-th normal mode is

$$c^{(2)}_{psp,q} = L_{zyx} c^{(2)}_{zyx,q} - L_{xyz} c^{(2)}_{xyz,q} \ ,$$

where L_{zyx} and L_{xyz} are the Fresnel factors, and $\chi^{(2)}_{ijk,q}$ (*i*, *j*, *k* = *x*, *y* or *z*, which is the lab coordinate) is the tensor element of the macroscopic second-order susceptibility of the interface. $\chi^{(2)}_{ijk,q}$ is defined by the vector sum of the microscopic vibrational hyperpolarizability for *q*-th normal mode $\beta_{lmn,q}$ (*l*, *m*, *n* = *a*, *b* or *c*, which is the molecular coordinate) *via* an Euler transformation:

$$c^{(2)}_{ijk,q} = N_s \sum_{l,m,n} \langle R_{il} R_{jm} R_{kn} \rangle \beta_{lmn,q} \ ,$$

where N_s is the number density of the chromophores, and $\langle R_{il} R_{jm} R_{kn} \rangle$ is the average product of the Euler transformation matrix for the projection from the molecular coordinate (*a*, *b* and *c*) onto the lab coordinate (*x*, *y*, and *z*). $\langle R_{il} R_{jm} R_{kn} \rangle$ is a function of the Euler angles ϕ, θ, and ψ that are defined in Fig. 2b of Ref. (42):

$$R = \begin{pmatrix} \cos(\varphi)\cos(\theta)\cos(\psi) - \sin(\varphi)\sin(\psi) & \cos(\varphi)\cos(\theta)\sin(\psi) + \sin(\varphi)\cos(\psi) & -\cos(\varphi)\sin(\theta) \\ -\sin(\varphi)\cos(\theta)\cos(\psi) - \cos(\varphi)\sin(\psi) & -\sin(\varphi)\cos(\theta)\sin(\psi) + \cos(\varphi)\cos(\psi) & \sin(\varphi)\sin(\theta) \\ \sin(\theta)\cos(\psi) & \sin(\theta)\sin(\psi) & \cos(\theta) \end{pmatrix}$$

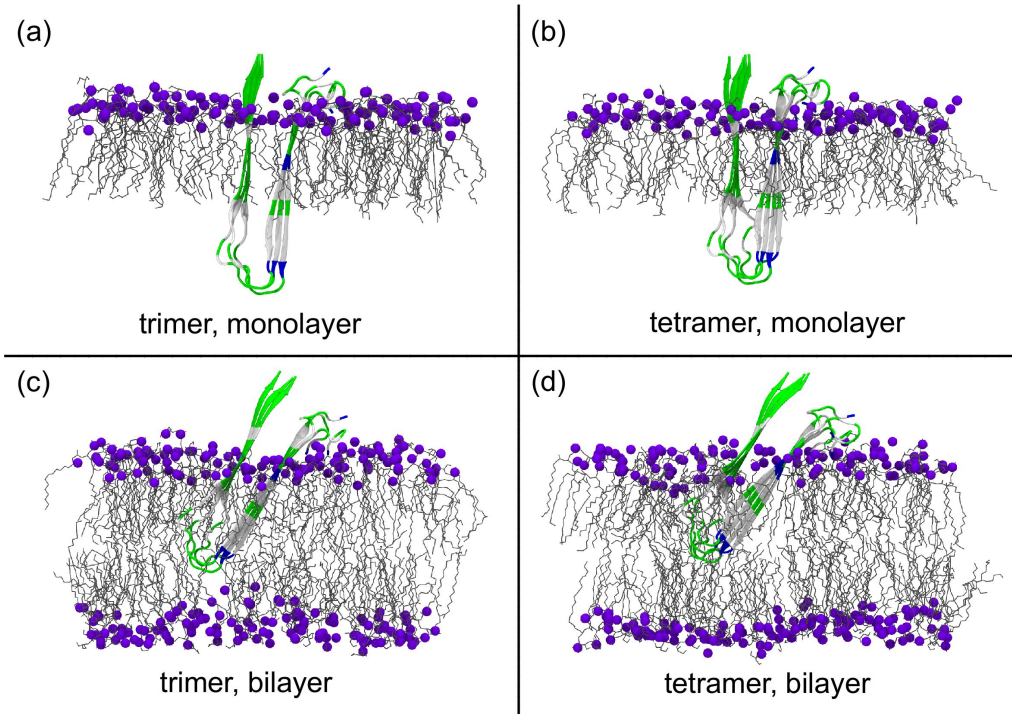

Figure S4: Starting structures showing the initial positions of hIAPP trimer and tetramer in both DPPG monolayer and bilayer.

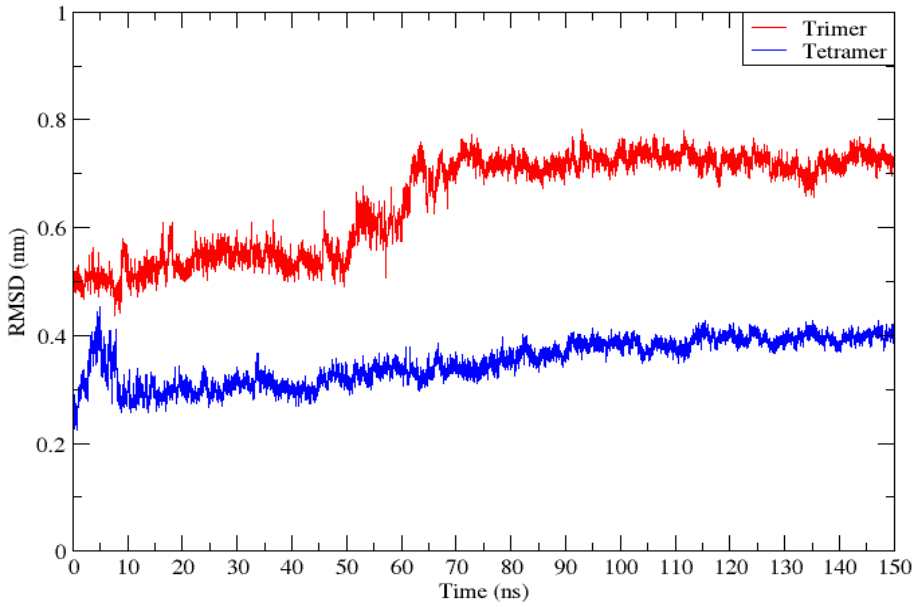

Figure S5: Backbone RMSD of hIAPP in DPPG monolayer.

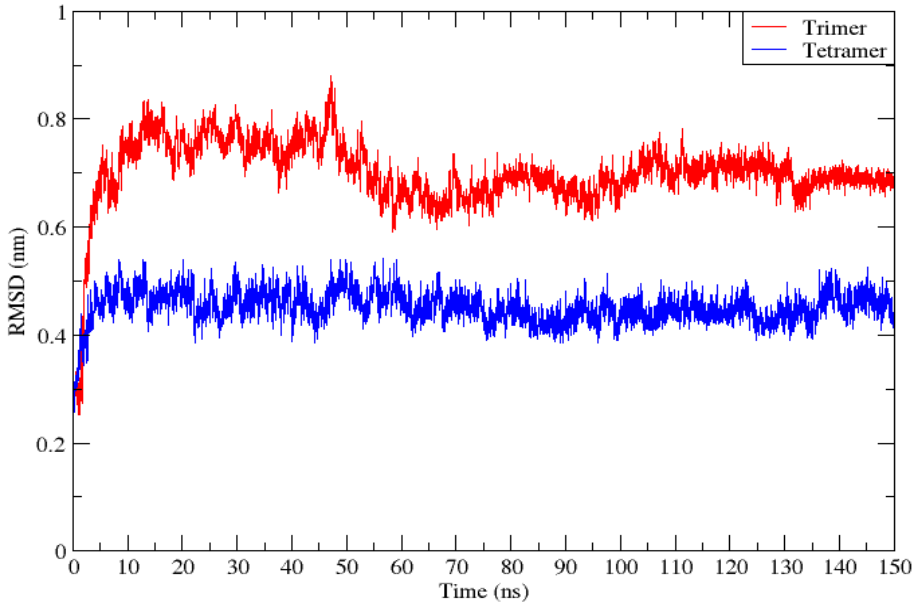

Figure S6: Backbone RMSD of hIAPP in DPPG bilayer.

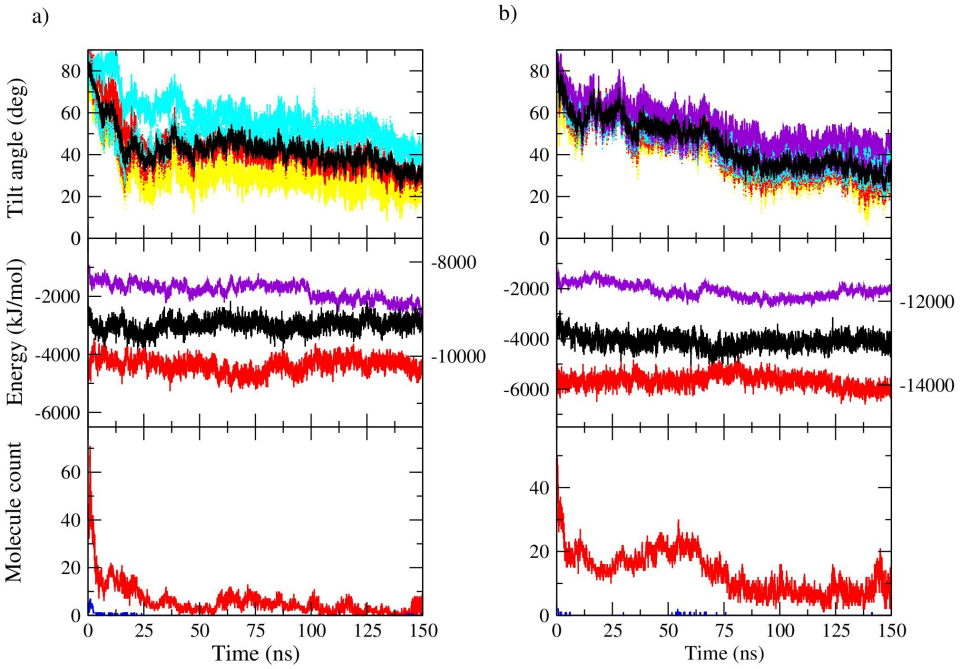

Figure S7: hIAPP in monolayer; (a) hIAPP trimer and (b) hIAPP tetramer. Top: Average (black) and individual tilt angles of β-strands relative to the membrane surface. Middle: Total interaction energies for hIAPP–lipid headgroups (purple), hIAPP–hIAPP (black, right *y*-axis), hIAPP–water/ions (red) interactions. Bottom: Number of water molecules (red) and Na^+ ions (blue) inside the hydrophobic core.

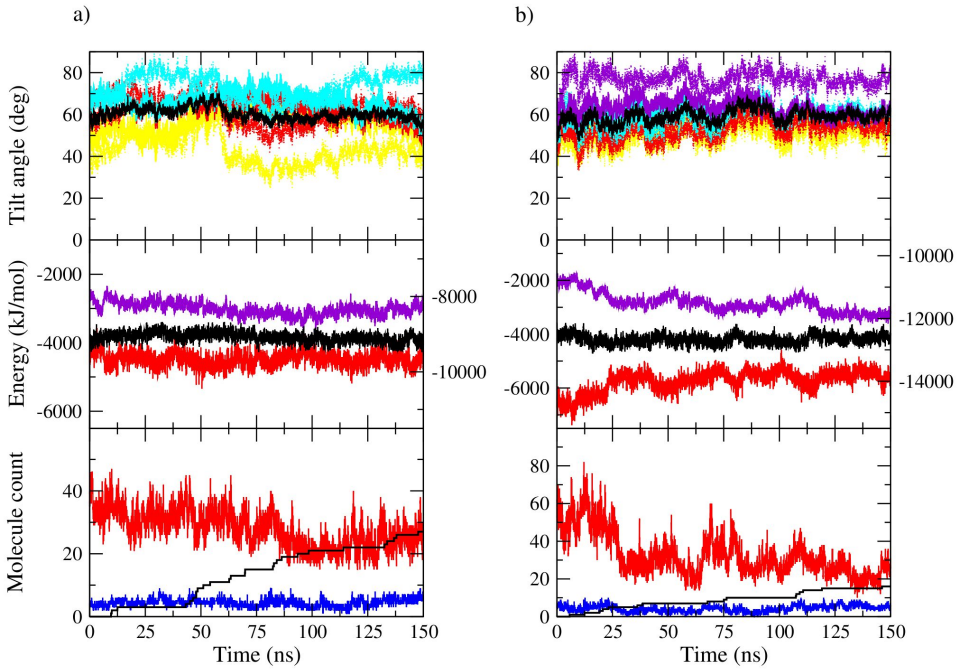

Figure S8: hIAPP in bilayer; (a) hIAPP trimer and (b) hIAPP tetramer. Top: Average (black) and individual tilt angles of β-strands relative to the membrane surface. Middle: Total interaction energies for hIAPP–lipid headgroups (purple), hIAPP–hIAPP (black, right *y*-axis), hIAPP–water/ions (red) interactions. Bottom: Number of water molecules (red) and Na^+ ions (blue) inside the hydrophobic core, as well as the cumulative number of water permeation events (black).

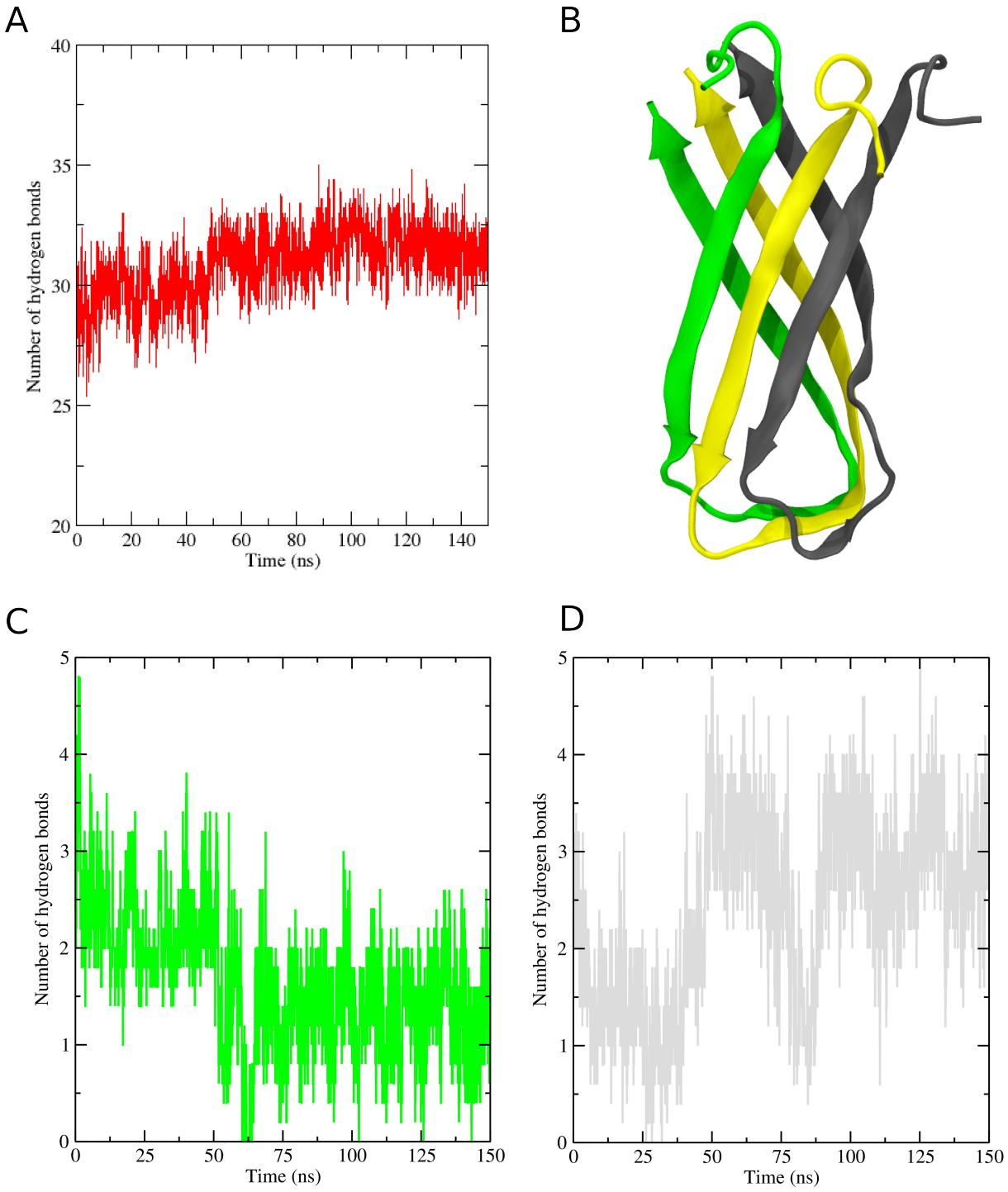

Figure S9: (a) Number of intra- and interpeptide hydrogen bonds in the hIAPP trimer in DPPG bilayer. (b) Most stable trimer structure colored by peptide numer (peptide 1, 2 and 3 in green, yellow and grey, respectively). (c) and (d) Number of H-bonds formed between the two β-sheets of peptide 1 (green) and peptide 3 (grey).

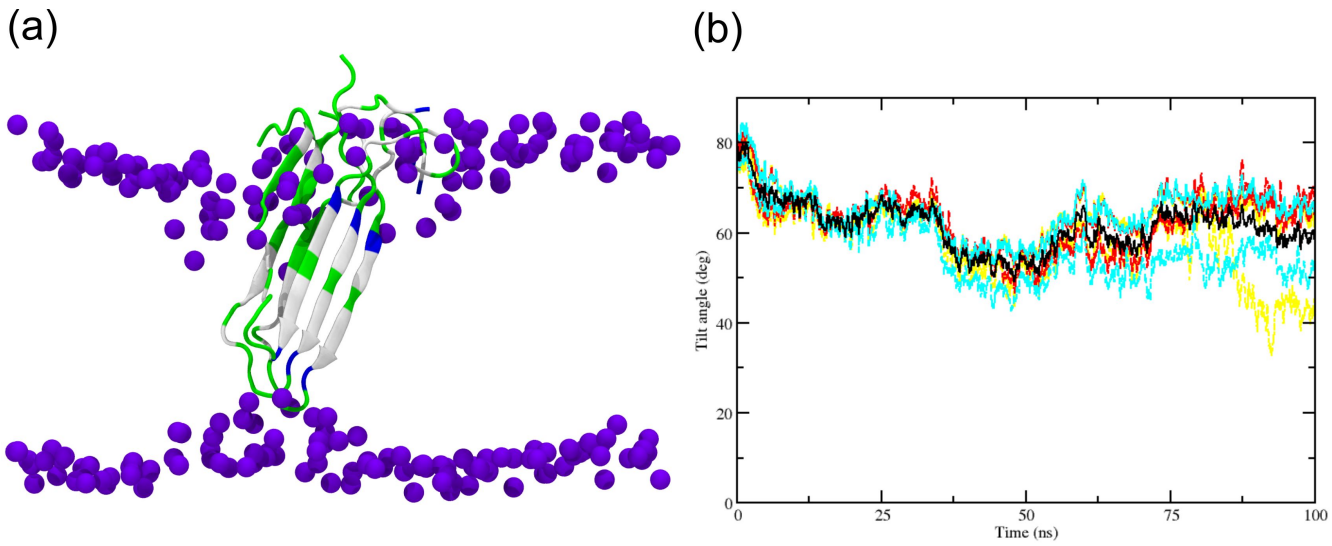

Figure S10: hIAPP trimer when inserted at 90^0 angle in a DPPG bilayer: (a) The most stable structure obtained from cluster analysis. (b) Average (dark line) and individual tilt angles of β strands relative to the membrane surface.

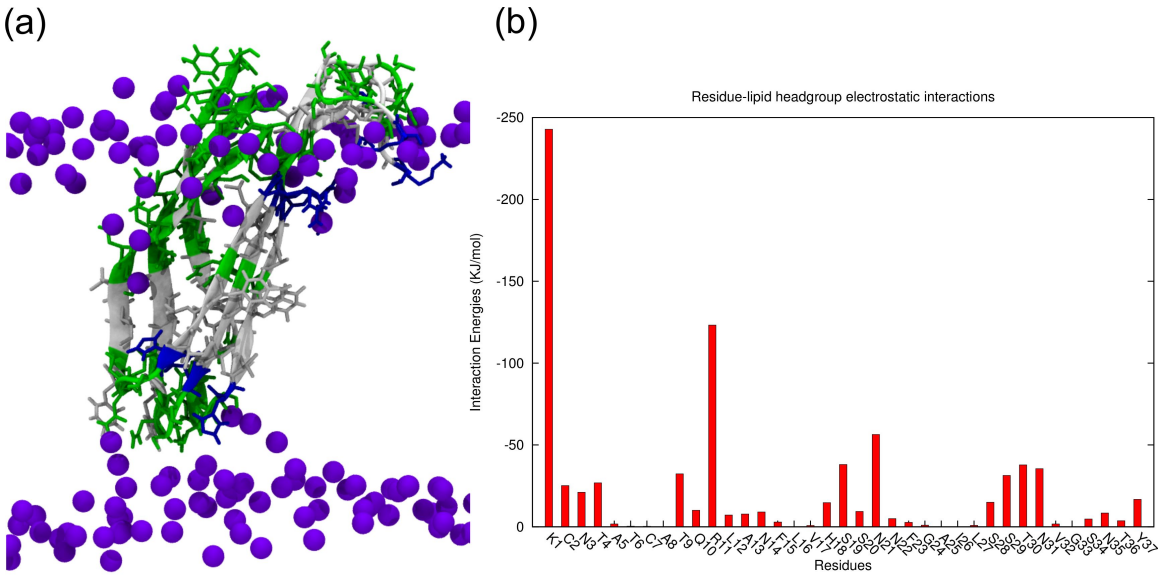

Figure S11: hIAPP trimer in a DPPG bilayer: (a) The most stable structure obtained from cluster analysis. The trimer side chains are shown as licorice. (b) Electrostatic interaction energies between the trimer residues and lipid headgroups. The interaction energies are averaged over three β strands.

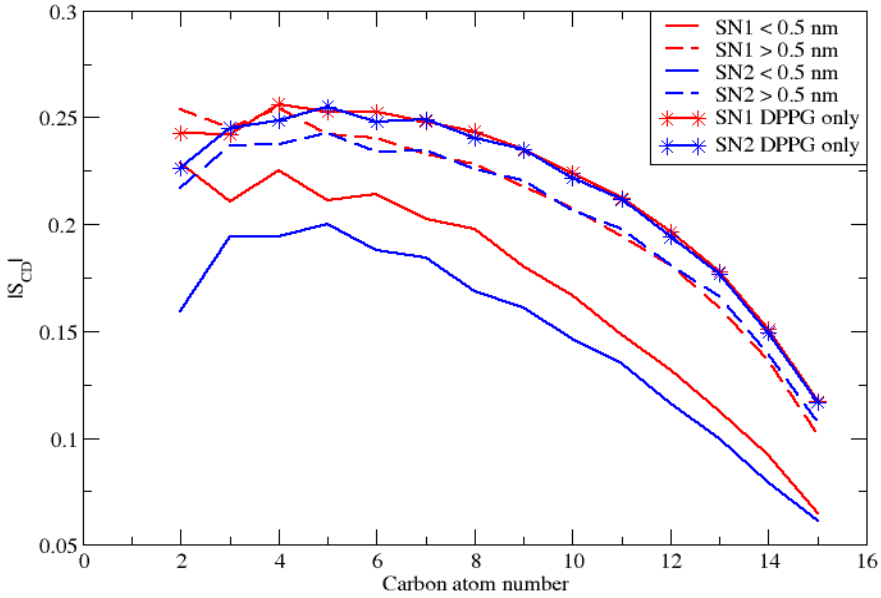

Figure S12: Time-averaged order parameter $|S_{CD}|$ of the sn-1 and sn-2 lipid chains resulting from the MD simulation of the hIAPP trimer in DPPG monolayer. S_{CD} is analyzed for lipids within 0.5 nm of protein and for lipids more than 0.5 nm away from protein. For comparison, $|S_{CD}|$ for lipids from the DPPG-only simulation is shown.

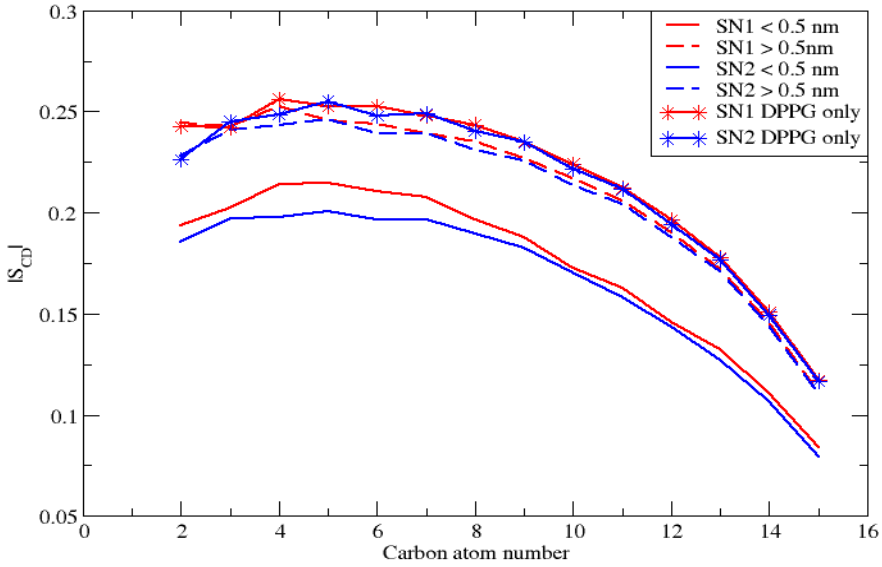

Figure S13: Time-averaged order parameter $|S_{CD}|$ of the sn-1 and sn-2 lipid chains resulting from the MD simulation of the hIAPP tetramer in DPPG monolayer. S_{CD} is analyzed for lipids within 0.5 nm of protein and for lipids more than 0.5 nm away from protein. For comparison, $|S_{CD}|$ for lipids from the DPPG-only simulation is shown.

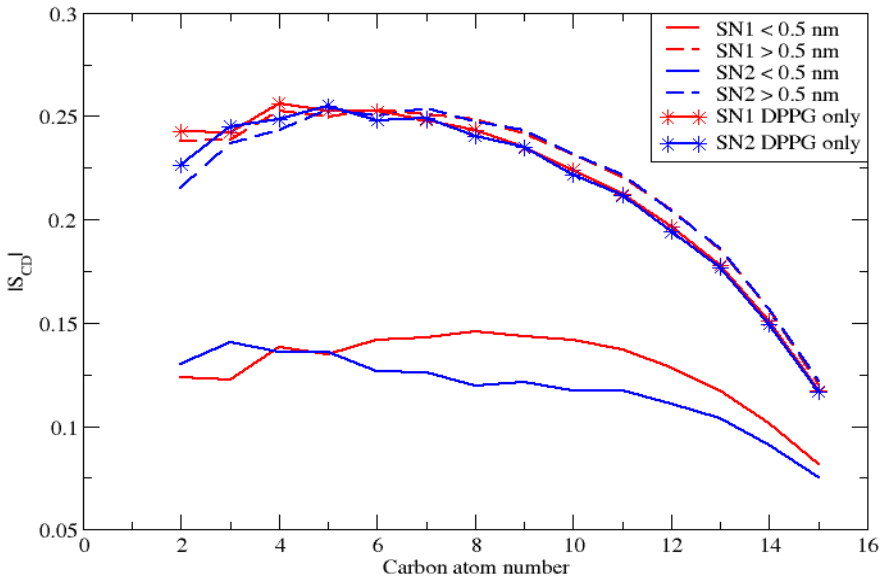

Figure S14: Time-averaged order parameter $|S_{CD}|$ of the sn-1 and sn-2 lipid chains resulting from the MD simulation of the hIAPP trimer in DPPG bilayer. S_{CD} is analyzed for lipids within 0.5 nm of protein and for lipids more than 0.5 nm away from protein. For comparison, $|S_{CD}|$ for lipids from the DPPG-only simulation is shown.

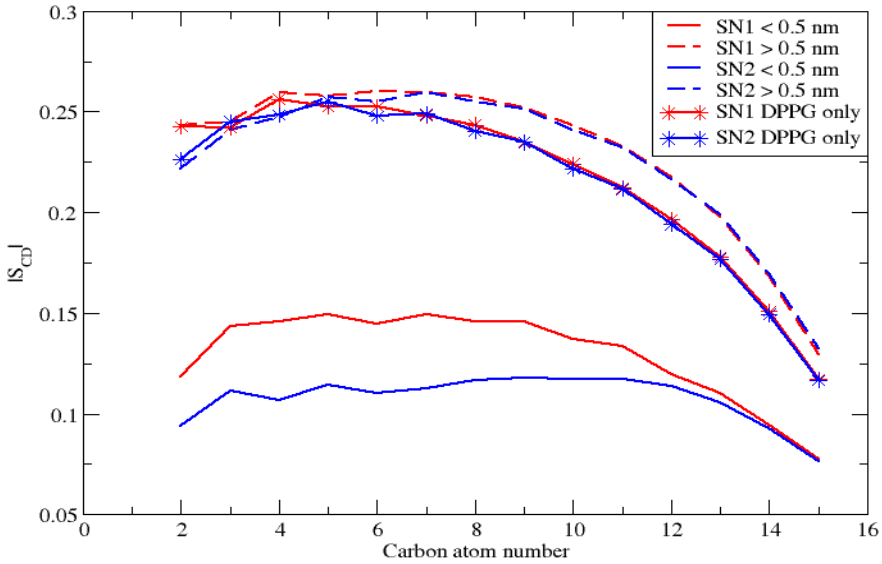

Figure S15: Time-averaged order parameter $|S_{CD}|$ of the sn-1 and sn-2 lipid chains resulting from the MD simulation of the hIAPP tetramer in DPPG bilayer. S_{CD} is analyzed for lipids within 0.5 nm of protein and for lipids more than 0.5 nm away from protein. For comparison, $|S_{CD}|$ for lipids from the DPPG-only simulation is shown.

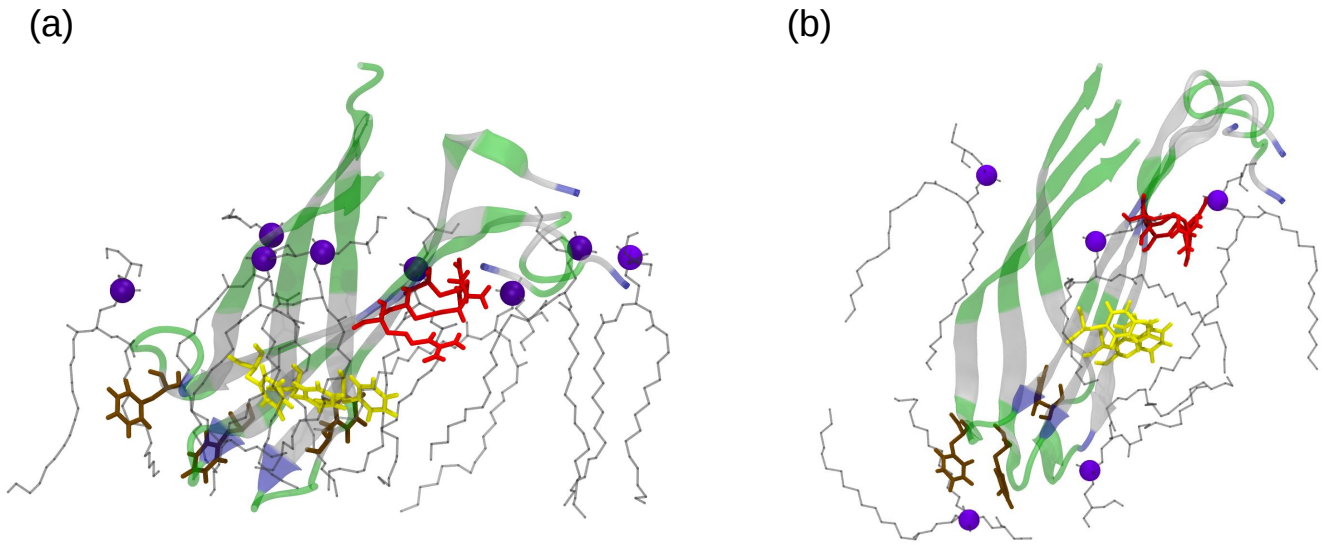

Figure S16: hIAPP trimer causing lipids in the (a) monolayer and (b) bilayer to tilt in the near vicinity of the peptides. The side chains with the strongest effect on acyl chain order are shown: Arg11 (red), Phe15 (yellow) and Phe23 (ochre).

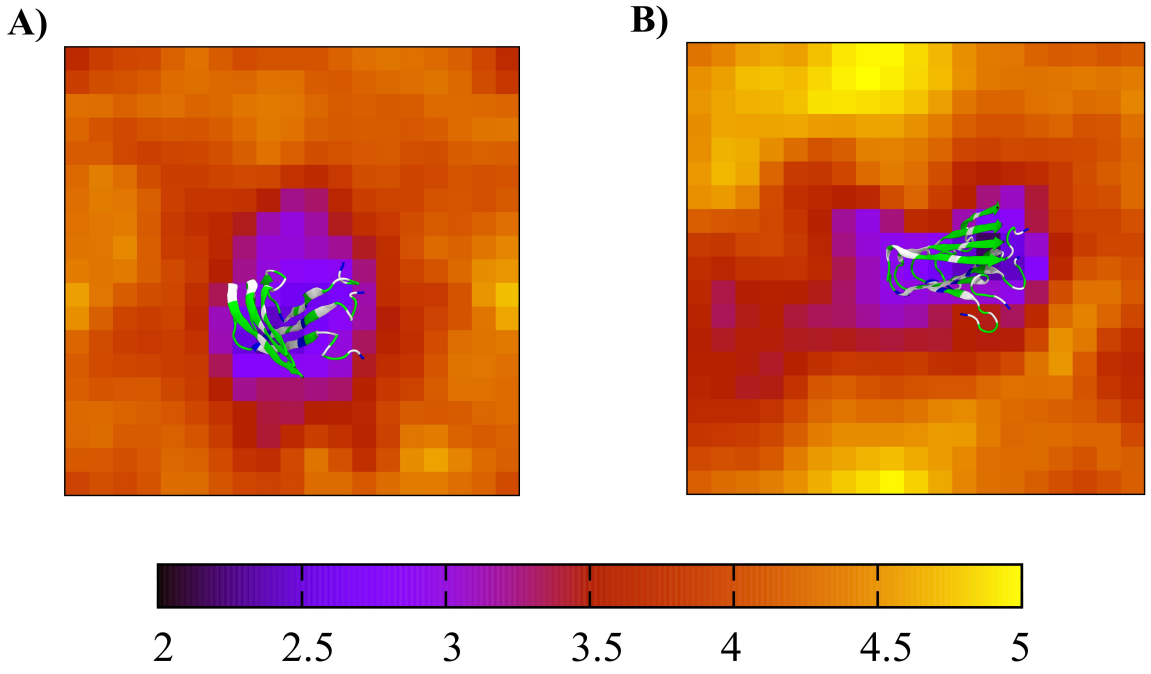

Figure S17: Bilayer thickness around embedded hIAPP for (a) trimer and (b) tetramer calculated for the final MD frame. For clarity, hIAPP was placed on the plots to indicate its position in the bilayer. The legend shows the bilayer thickness (nm) mapped to the corresponding colors.

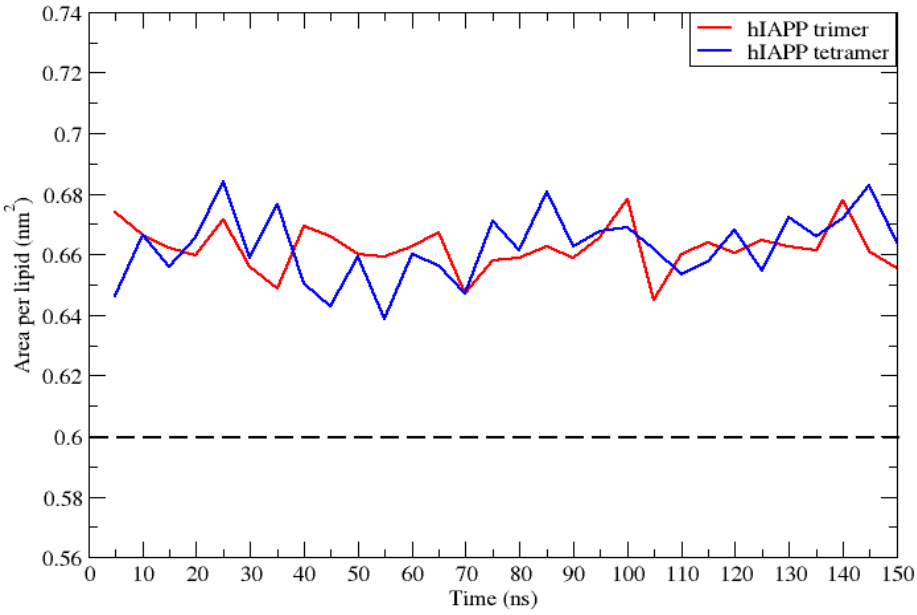

Figure S18: Area per lipid as a function of time for the DPPG monolayer simulations with hIAPP trimer (red) and tetramer (blue). For comparison, the average area per lipid obtained from a peptide-free DPPG bilayer is shown as black dashed line.

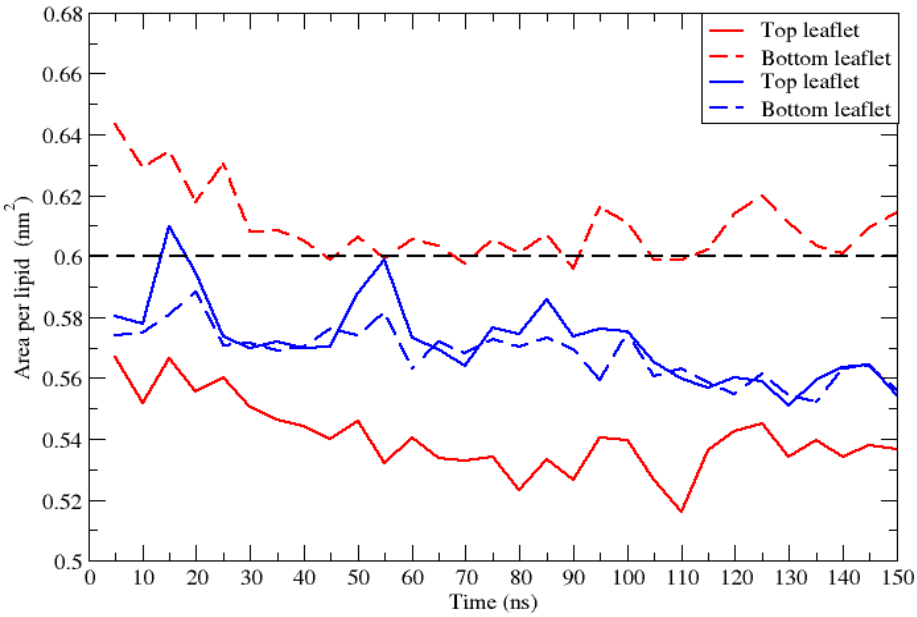

Figure S19: Area per lipid as a function of time for the DPPG bilayer simulations with hIAPP trimer (red) and tetramer (blue). For comparison, the average area per lipid obtained from a peptide-free DPPG bilayer is shown as black dashed line.

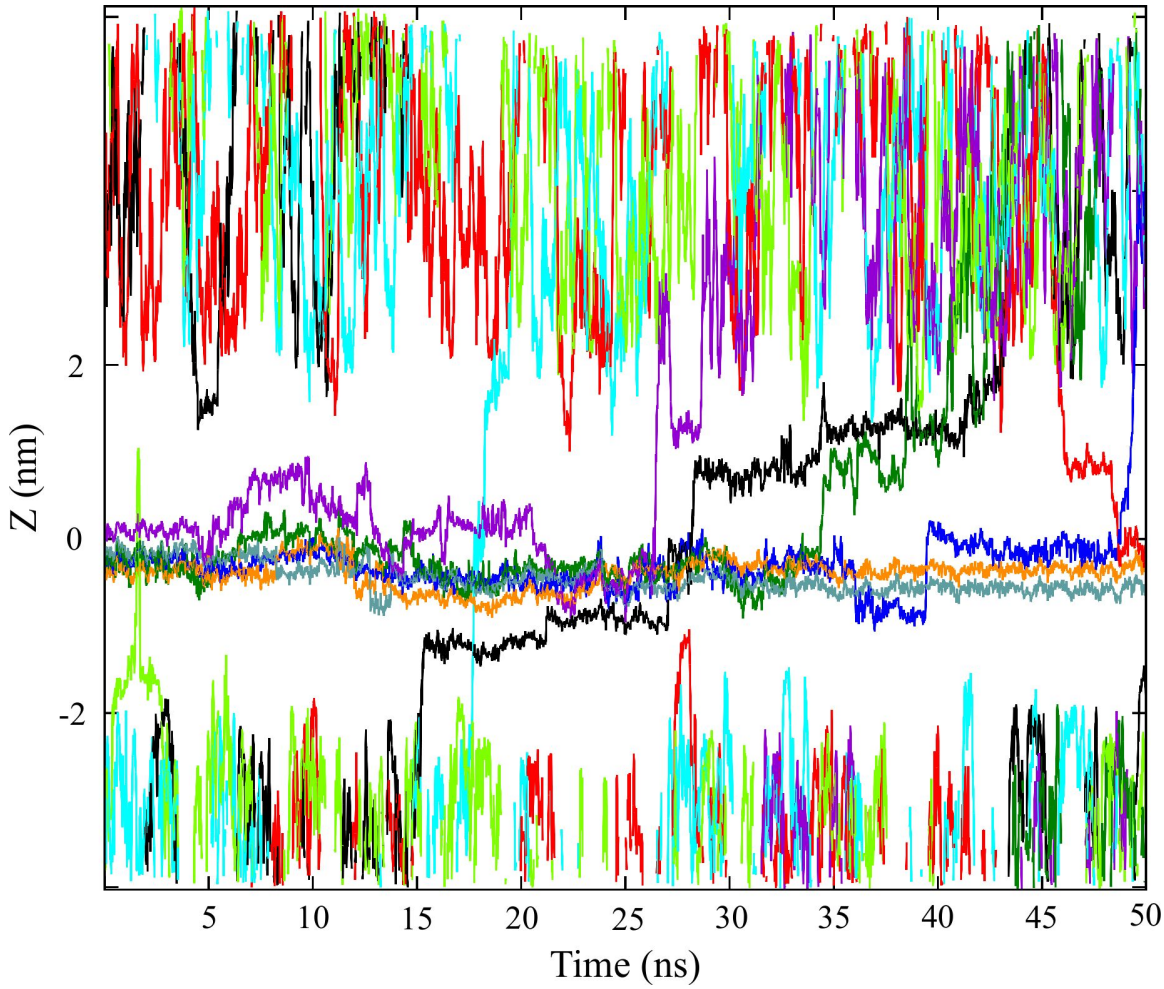

Figure S20: Representative trajectories of water molecules permeating the DPPG bilayer with hIAPP trimer inserted. Only the coordinate along the bilayer normal (*z*-axis) is plotted, and only permeation events occurring during the last 50 ns of the 150 ns MD simulation are shown.

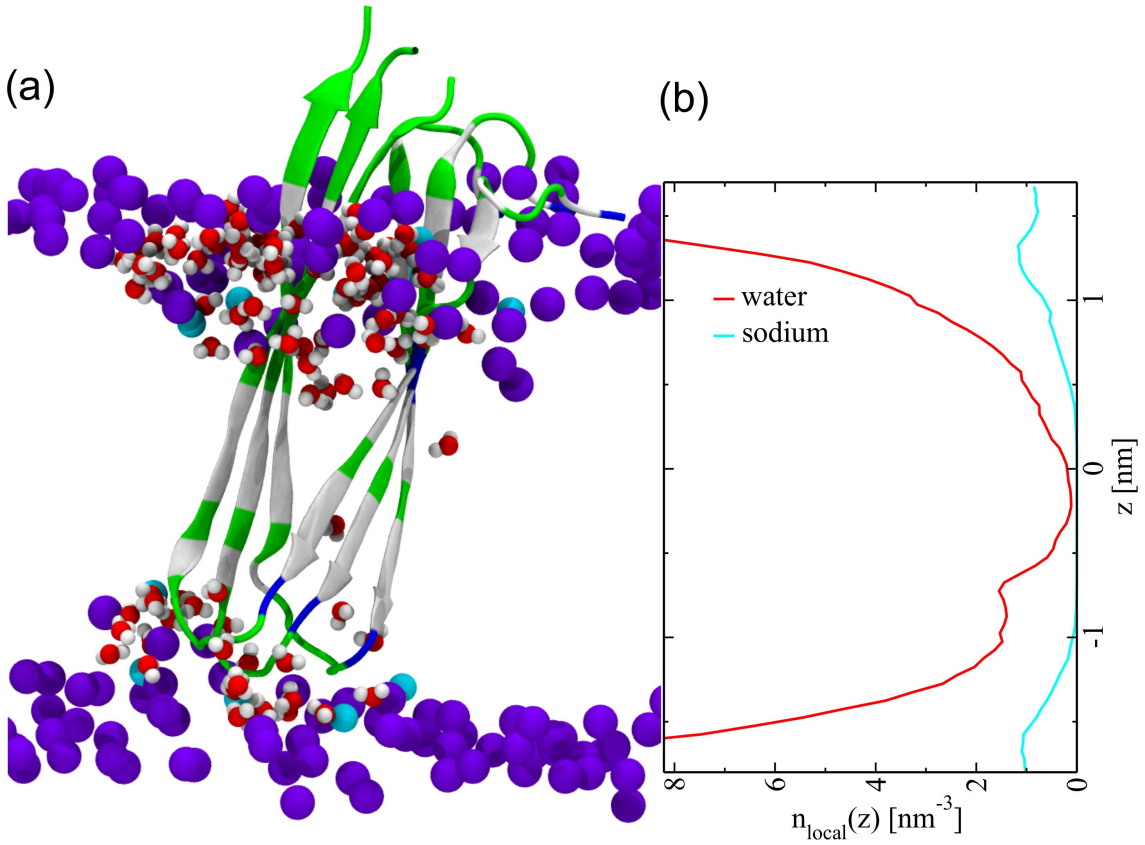

Figure S21: hIAPP trimer in a DPPG bilayer**:** (a) The most stable structure obtained from cluster analysis. The figure shows reduced water flow into the membrane and ions do not diffuse into the membrane hydrophobic core. Water molecules and Na^+ are shown as vdW spheres. (b) Averaged particle density of water and Na^+ within the the bilayer.

SUPPORTING REFERENCES

1. Martinez, L., R. Andrade, E. G. Birgin, and J. M. Martinez, 2009. PACKMOL: A Package for Building Initial Configurations for Molecular Dynamics Simulations. *J. Comput. Chem*. 30:2157–2164.

2. Feller, S. E., Y. Zhang, and R. W. Pastor, 1995. Computer simulation of liquid/liquid interfaces. II. Surface tension–area dependence of a bilayer and monolayer. *J. Chem. Phys*. 103:10267–10276.

3. Baoukina, S., Mendez-Villuendas, E, and Tieleman, P. D, 2012. Molecular view of phase coexistence in lipid monolayers. *J. Am. Chem. Soc*. 134:17543–17553.

4. Xiao, D., L. Fu, J. Liu, V. S. Batista, and E. C. Yan, 2012. Amphiphilic Adsorption of Human Islet Amyloid Polypeptide Aggregates to Lipid/Aqueous Interfaces. J. Mol. Biol. 421:537 – 547.